Sādhanā Vol. 29, Part 1, February 2004, pp. 117–127. © Printed in India

The role of graphite morphology and matrix structure on low frequency thermal cycling of cast irons

S Y BUNI, N RAMAN and S SESHAN

Department of Mechanical Engineering, Indian Institute of Science, Bangalore 560 012, India
e-mail: seshan@mecheng.iisc.ernet.in

MS received 14 August 2002; revised 23 November 2002

Abstract. Low frequency thermal cycling tests were carried out on four types of cast iron (viz., austempered ductile iron, pearlitic ductile iron, compacted/vermicular graphite iron and grey cast iron) at predetermined ranges of thermal cycling temperatures. The specimens were unconstrained.

Results show that austempered ductile iron has the highest thermal cycling resistance, followed by pearlitic ductile iron and compacted graphite iron, while grey cast iron exhibits the lowest resistance. Microstructural analysis of test specimens subjected to thermal cycling indicates that matrix decomposition and grain growth are responsible for the reduction in hardness while graphite oxidation, de-cohesion and grain boundary separation are responsible for the reduction in the modulus of elasticity upon thermal cycling.

Keywords. Thermal cycling resistance; graphite morphology; grey cast iron; austempered ductile iron; compacted/vermicular graphite iron; matrix decomposition.

1. Introduction

When a material is subjected to a temperature gradient, it tends to expand differentially. During this process, thermal stresses are induced. The source of heat that causes the thermal gradient may be friction as in the case of brake drums, or external media as in the case of cylinder heads. When thermal stresses are generated by changes in temperature, thermal shock or thermal fatigue is the result. Two types of thermal cycles are possible.

(i) Low frequency thermal cycle in which the time taken for completion of the cycle is large enough to cool the component. Typical examples are ingot moulds and brake drums of railway coaches.
(ii) High frequency thermal cycle in which the time involved is in milli-seconds and the heating and cooling are influenced by the thermal inertia of the system under consideration. Cylinder heads, piston rings and exhaust manifolds are standing examples of components which experience high frequency thermal cycles.

2. Failure due to thermal cycling

According to Roehrig (1978), metallic components subjected to thermal cycling/thermal fatigue may fail in one of the following ways.

(i) *Type 1 failure:* Cracks appear first on the hot zone of the component (in the heat-checking net work) and may eventually propagate through the section. This is the most common type of failure observed in grey cast irons and other brittle materials.
(ii) *Type 2 failure:* Severe distortion which ultimately renders the component useless. This type of failure is usually found in ductile iron components.
(iii) *Type 3 failure:* Gross cracking through the entire section during the first few cycles. These failures emanate due to the mismatching of materials selected, improper design and random thermal cycling.
(iv) *Type 4 failure:* Lowering of mechanical properties of materials due to metallurgical variations such as microstructural changes and internal oxidation, which can lead to premature failure of components.

3. Factors affecting thermal fatigue resistance

To resist thermal fatigue, the material selected for a constrained component should have the following properties (some of the requirements may be relaxed for an unconstrained member).

(i) High thermal conductivity.
(ii) High elastic limit or high tensile strength and a narrow stress/strain hysteresis loop.
(iii) Low creep in compression.
(iv) High mechanical fatigue strength under conditions of repeated plastic strain.
(v) High ductility.
(vi) Resistance to internal and external oxidation.
(vii) Resistance to microstructural changes.
(viii) Elevated temperature properties, especially tensile strength.
(ix) Low coefficient of thermal expansion.

4. Earlier work on thermal fatigue resistance of cast irons

Literature dealing with cast irons indicates that the thermal fatigue resistance of cast irons can be improved by one of the following methods.

(i) By judicious alloying (Dearden 1961; Gundlach 1978, 1979; Roehrig 1978; Park *et al* 1985; Dawson & Sage 1989)
(ii) By changing the morphology of graphite in cast irons (Drapkin *et al* 1973; Roehrig 1978; Rukadikar & Reddy 1987)
(iii) By increasing the carbon content (Roehrig 1978; Shea 1978; Rukadikar & Reddy 1987)
(iv) By thermal shielding of components (Dearden 1961)

The literature review further indicates that although details are available on low frequency thermal cycling tests on constrained cast iron specimens (of different graphite morphology

Table 1. Mechanical properties of cast irons investigated.

Material	UTS (MPa)	E (GPa)	Hardness (BHN)	Fracture toughness (MPa.m$^{1/2}$)
Austempered ductile iron	1240	170	375	69·5
Pearlitic ductile iron	723	164	285	37·5
Compacted graphite iron	512	152	230	31·4
Grey cast iron	220	141	200	19·1

and matrix microstructure), the same cannot be said about unconstrained specimens. One such unconstrained component is the piston ring of IC engines. The ring is free to expand both in the circumferential and axial directions. Reduction of friction due to lubrication more or less eliminates the possibility of constraining the surfaces of rings against the counter surfaces of piston and cylinder liner, thus leading to unconstrained conditions.

In order to generate data pertaining to such situations, the investigation reported here was taken up on cast iron specimens. The resistance to thermal cycling of four types of cast iron with dissimilar graphite morphology and matrix microstructures has been assessed experimentally under unconstrained conditions. Subsequently, the attributes of some of the important mechanical properties (viz., modulus of elasticity and hardness) are analysed.

5. Experimental details

5.1 *Cast irons evaluated in this work*

For studying the resistance to thermal cycling, four different types of cast irons (viz. austempered ductile iron, normal, pearlitic ductile iron, compacted graphite iron and grey cast iron) were selected. The mechanical properties of these cast irons were first assessed (table 1).

5.2 *Assessment of thermal fatigue resistance*

In the absence of standard equipment, a facility to meet the requirements was designed and fabricated exclusively for this work. The schematic diagram of the unit is shown in figure 1. The unit consisted of a tubular furnace, a portable air blower, a circular specimen holder and a control unit to regulate the higher and lower cycle temperatures. The test was commenced by heating the specimens inside the furnace to the desired test temperature and maintaining the temperature at predetermined levels (300°, 500°, 600° and 700°C respectively). When the upper level of temperature was reached, the regulator turned on the blower, which pumped in air in order to bring down the temperature rapidly. As the temperature of the specimen came down to the lower level of the cycle temperature, the regulator put off the blower, allowing the specimen to heat up again.

The samples were taken out from the furnace after they have undergone the pre-determined number of thermal cycles and were evaluated for change in properties. Details pertaining to the above trials are given in table 2.

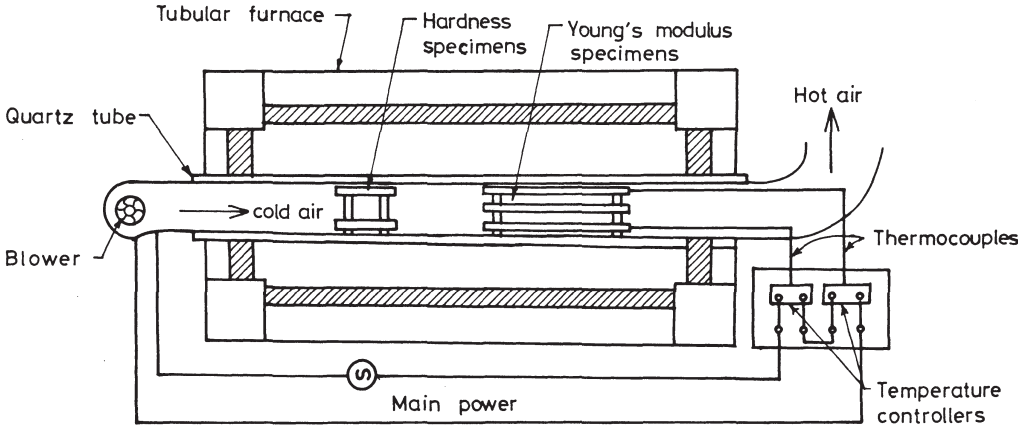

Figure 1. Schematic diagram of low frequency thermal cycling test rig (Buni 1994).

The reason for keeping the lower temperature at 120°C is to prevent the moisture in the atmosphere from condensing on the specimens. The thermal cycle 120–500°C has some special significance in that the surface temperatures of components like piston rings and exhaust manifolds are expected to be around 500°C. The hardness and Young's modulii were measured periodically. Any change in the microstructure was recorded at the end of the thermal cycling trials. The investigations pertained to the doctoral thesis work of Buni (1994).

6. Results and discussion

6.1 *Variation of hardness on thermal cycling*

The effect of thermal cycling on hardness is illustrated in figure 2a and b and 3a and b. There is a rapid nonlinear reduction in hardness up to 1000 cycles. Afterwards, there appears to be a linear relation between hardness and the number of thermal cycles. The rate of decrease in hardness is more in the case of ductile irons (viz. austempered ductile iron and pearlitic ductile iron) than in the case of interconnected graphite irons (C G iron and grey iron). Superior thermal conductivity and thermal diffusivity of flake graphite and compacted graphite irons could be responsible for this slow reduction. However, since room temperature hardness of ductile irons is much higher than that of grey and compacted graphite irons, ductile irons occupy higher positions in the plots.

Table 2. Details of thermal cycling.

Thermal cycle range (°C)	Heating time (s)	Cooling time (s)	No. of cycles (for assessing BHN)	No. of cycles (for assessing E)
120–300	120	50	3000	6000
120–500	254	120	6000	9800
120–600	320	160	5000	5000
300–750	266	133	1500	1500

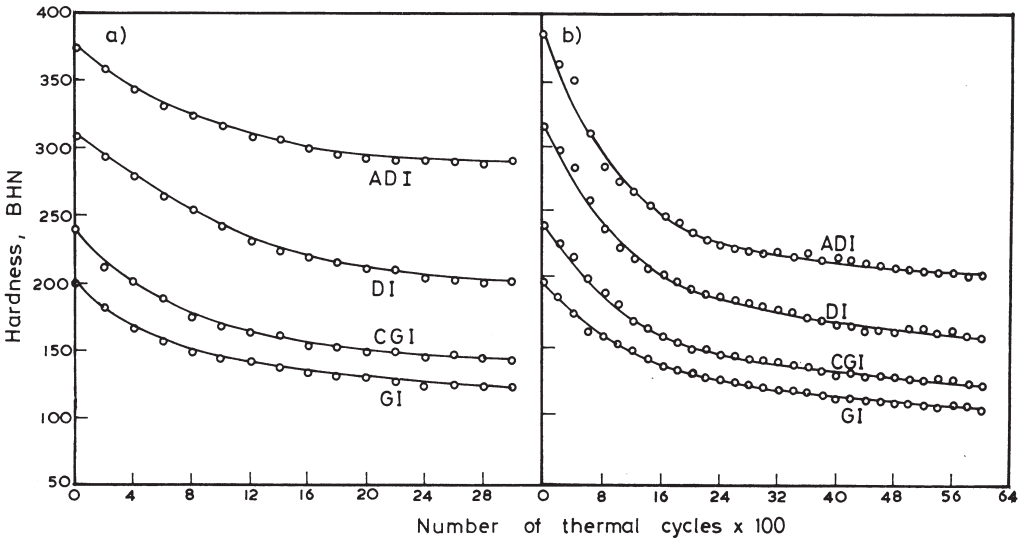

Figure 2. Variation of hardness with number of thermal cycles (Buni 1994). ADI – austempered ductile iron; DI – spheroidal ductile iron; CGI – compacted graphite iron; GI – grey iron. Thermal cycle range: **(a)** 120–300°C **(b)** 120–500°C.

This means that the morphology of graphite plays an important role in the deterioration of the strength during thermal cycling. Inferior thermal conductivity of ductile irons may lead to the presence of localised hot zones within the material during thermal cycling. Hence, more decomposition of matrix is expected in ductile irons than in flake irons with the consequent lowering of hardness.

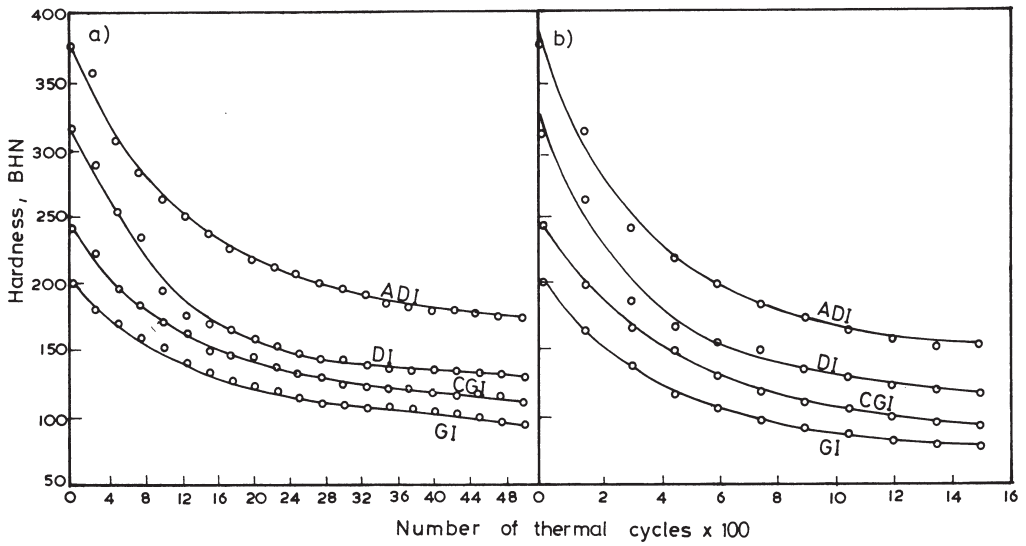

Figure 3. Variation of hardness with number of thermal cycles (Buni 1994). ADI – austempered ductile iron; DI – spheroidal ductile iron; CGI – compacted graphite iron; GI – grey iron. Thermal cycle range: **(a)** 120–600°C **(b)** 300–750°C.

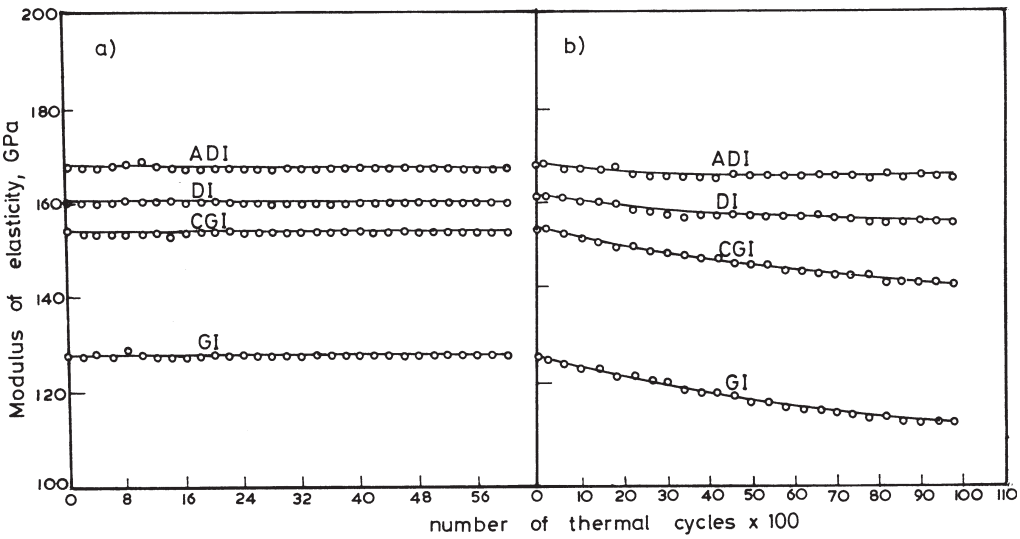

Figure 4. Variation of modulus of elasticity with number of thermal cycles (Buni 1994). ADI – austempered ductile iron; DI – spheroidal ductile iron; CGI – compacted graphite iron; GI – grey iron. Thermal cycle range: **(a)** 120–300°C **(b)** 120–500°C.

6.2 *Variation of elastic modulus on thermal cycling*

The effect of thermal cycling on Young's modulus is shown in figures 4a and b and 5a and b. There is hardly any change in the value of Young's modulus with the number of thermal

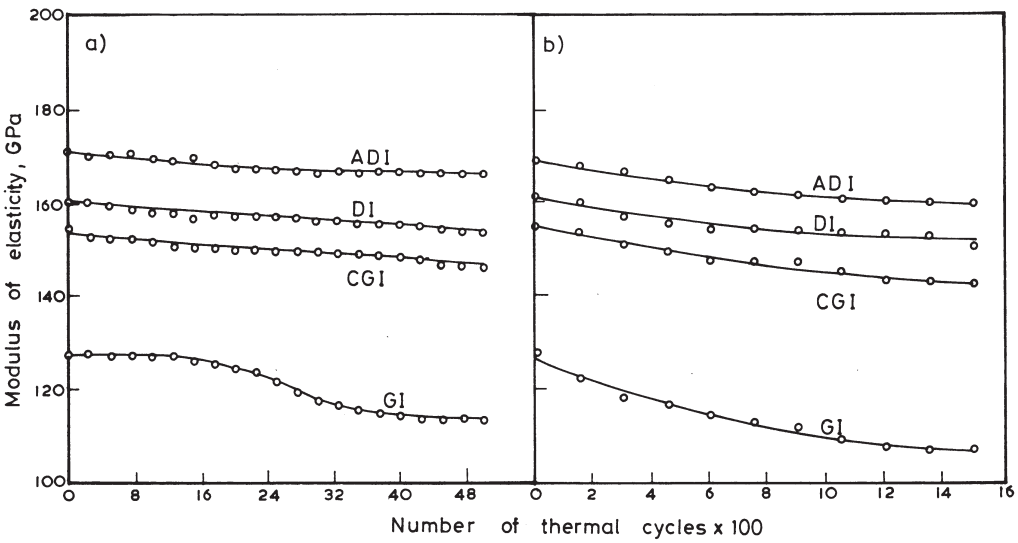

Figure 5. Variation of modulus of elasticity with number of thermal cycles (Buni 1994). ADI – austempered ductile iron; DI – spheroidal ductile iron; CGI – compacted graphite iron; GI – grey iron. Thermal cycle range: **(a)** 120–160°C **(b)** 300–750°C.

cycles for the temperatures range 120–300°C, probably due to the negligible oxidation of the graphite phase at this temperature. At higher temperature ranges, there is reduction in elastic modulus.

Changes in the graphite phase appear to be responsible for the above reduction of elastic modulus values. Oberle (1951) has considered the graphite phase as a hole in the matrix while explaining the lower values of elastic modulus of cast irons when compared to steels. The variation in the values of Young's modulus of different irons can then be explained on the basis of the shape of graphite and its effect on stress concentration. Naturally, ductile irons have a higher Young's modulus than interconnected graphite irons.

The reduction in Young's modulus corresponding to higher thermal cycling temperatures can be explained based on two grounds. One is the oxidation of the graphite phase. This oxidation reduces the bond between the matrix and graphite, resulting in the creation of holes. Since the perimeter length of interconnected graphite is more than that of nodular graphite, oxidation of graphite in compacted graphite iron and grey iron is more than for ADI and ductile iron. Further, only the surface graphite is oxidized in the case of ADI and ductile iron since the graphite nodules are divorced from each other. Interconnected graphite provides one continuous path for oxidation. Furthermore, any crack initiated in nodular graphite is limited to that nodule only whereas the cracks can propagate to any part of graphite in the case of compacted graphite iron and grey iron.

It is thus obvious that the susceptibility of interconnected graphite to greater oxidation and crack propagation is responsible for large reduction in the Young's modulus. During the initial stages of thermal cycling, the rate of reduction in hardness is greater in ADI and ductile iron than in compacted graphite iron and grey iron, but the rate of reduction in Young's modulus is less for ADI and ductile iron than in compacted graphite iron and grey iron. During the later part of the thermal cycling, the reduction of hardness and Young's modulus appears to be identical for all the irons.

6.3 *Microstructural changes on thermal cycling*

6.3a *Matrix decomposition:* Matrix decomposition here refers to the transformation of bainite and pearlite into ferrite. Figure 6 shows the partial transformation of pearlite in the

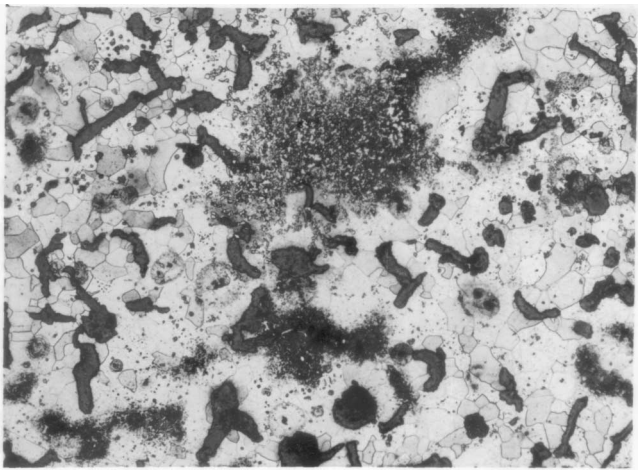

Figure 6. Partial transformation of pearlite in compacted graphite iron (thermal cycle range: 120–500°C).

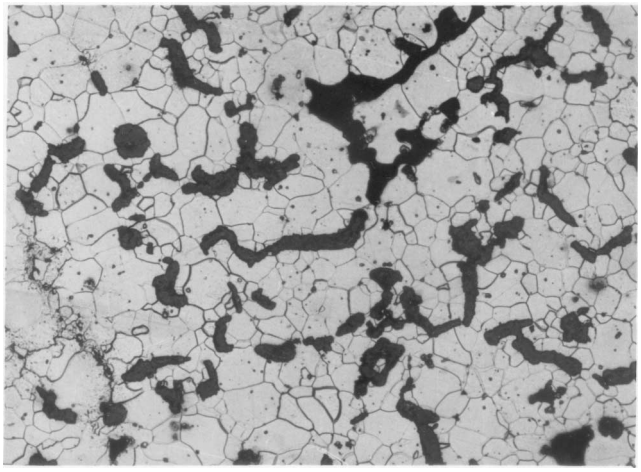

Figure 7. Full transformation of pearlite in compacted graphite iron (thermal cycle range: 120–600°C).

compacted graphite iron into ferrite, consequent to thermal cycling between 120–500°C. Similar decomposition of the matrix into ferrite was observed in the other types of cast irons also. Figure 7 shows the full transformation of pearlite into ferrite in compacted graphite iron. These transformations reduce the hardness but not the Young's modulus.

6.3b Graphite separation: Separation of graphite from the matrix was observed when the upper cycle temperature was increased to 500°C. This may be attributed to the surface oxidation of the graphite phase and the de-cohesion of graphite from the matrix due to the effect of continuously changing differential thermal expansion of graphite and the matrix. Figures 8 and 9 are the high magnification microstructures of ADI and ductile iron after thermal cycling. In addition to graphite separation, one can see cracks in the graphite phase (figure 9). This is also true for compacted graphite and grey cast irons. The matrix-graphite separation in

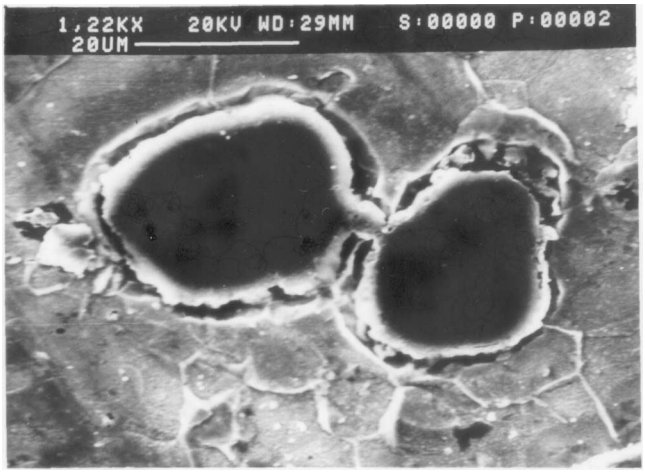

Figure 8. Graphite separation in austempered ductile iron (thermal cycle range: 120–500°C).

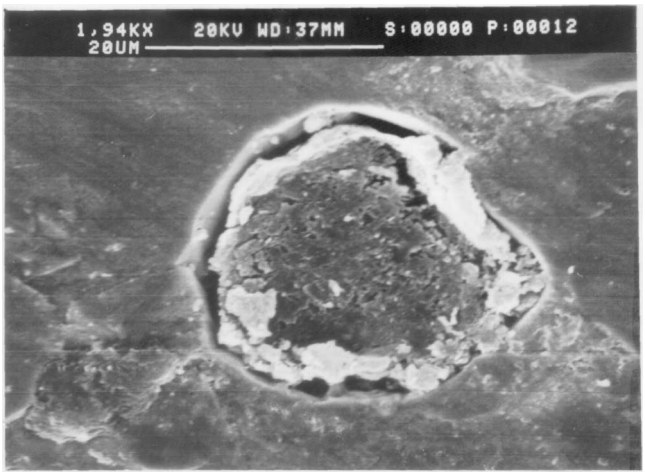

Figure 9. Graphite separation in spheroidal graphite iron (thermal cycle range: 120–500°C).

grey cast iron is seen clearly in figure 10. The additional space between the graphite and the matrix is responsible for lowering the Young's modulus value, since less stress is required to produce additional strains.

6.3c *Grain growth and grain boundary separation:* Lowering of hardness is also partially due to matrix grain growth. Larger grains provide additional space for the movement of dislocations before they are pinned at grain boundaries. Ease of movement of dislocation means reduced hardness. Figure 11 shows the phenomenon of grain boundary separation in ductile iron after thermal cycling in the range of 120–600°C. Such grain boundary separation is bound to produce premature failure of specimens under cyclic mechanical and cyclic thermal loading. All the above changes are observed when the upper limit of thermal cycling was 500°C or above, whereas no appreciable change in microstructure of irons is observed at 120–300°C.

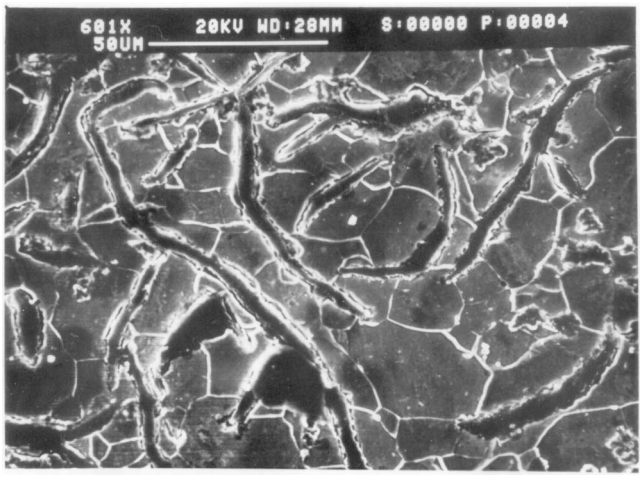

Figure 10. Matrix graphite separation in grey cast iron (thermal cycle range: 120–600°C).

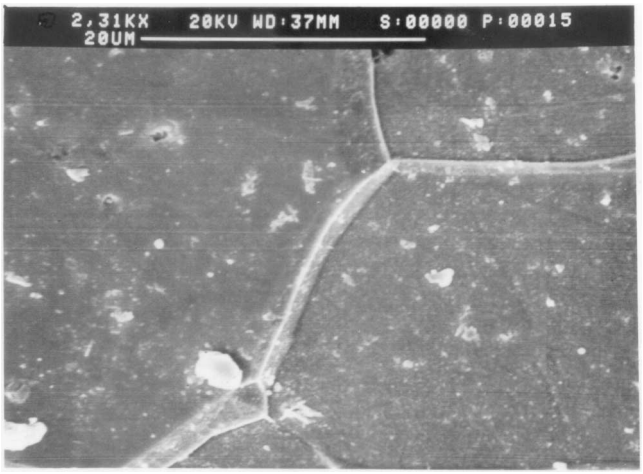

Figure 11. Grain boundary separation in spheroidal graphite iron (thermal cycle range: 120–600°C).

7. Conclusions

(1) The four cast irons investigated (viz. ADI, pearlitic ductile iron, compacted graphite iron and grey iron) react differently to thermal cycling. ADI has the highest thermal cycling resistance followed by ductile iron and compacted graphite iron, while grey cast iron exhibits the lowest resistance.
(2) Matrix decomposition and grain growth resulting from thermal cycling seem to be the causes for the reduction in the hardness in all cast irons.
(3) Oxidation of graphite, decohesion of graphite from the matrix and grain boundary separation contribute to lowering of Young's modulus values of the different cast irons subjected to thermal cycling
(4) The higher mechanical properties of ADI and ductile iron are partially responsible for their higher resistance to thermal cycling when compared to compacted graphite iron and grey cast iron.

References

Buni S Y 1994 *Investigation of wear and thermal cycling characteristics of cast irons with dissimilar forms of graphite*. Ph D thesis, Indian Institute of Bangalore, Bangalore

Dawson J V, Sage A M 1989 High strength cast irons containing vanadium annealed ductile irons and high carbon grey irons. *Foundryman* Oct: 479–489

Dearden A 1961 Residual thermal stresses in compression ignition engines. *BCIRA J.* 9: 540–559

Drapkin B M, Zhukov A A, Piguzov Y V 1973 The initial stage in thermal fatigue failure of cast iron. *Met. Sci. Heat Treatment* 15: 964–966

Gundlach R B 1978 Elevated temperature properties of alloyed gray irons for diesel engine components. *AFS Trans.* 86: 55–64

Gundlach R B 1979 Thermal Fatigue resistance of alloyed gray irons for diesel engine components. *AFS Trans.* 87: 551–560

Oberle T L 1951 Properties influencing wear of metals. *J. Metals* 3: 438–439

Park Y J, Gundlach R B, Thomas R G, Janowak J F 1985 Thermal fatigue resistance of gray and compacted graphite irons. *AFS Trans.* 93: 415–422

Roehrig K 1978 Thermal fatigue of gray and ductile irons. *AFS Trans.* 86: 75–88

Rukadikar M C, Reddy G P 1987 Thermal fatigue resistance of alloyed, pearlitic flake, graphite irons. *Int. J. Fatigue* 9: 25–34

Shea M M 1978 Influence of composition and microstructure on thermal cracking of gray cast iron. *AFS Trans.* 86: 23–30

Shikida M, Matsumoto H, Sakane M, Ohnami M 1991 High temperature low-cycle fatigue of flake, compacted vermicular and spheroidal graphite cast iron. *Nippon Kikai Gakkai Ronbushu* A57: 700–707 (in Japanese)